Desalination and Water Treatment
www.deswater.com

doi: 10.5004/dwt.2017.20501

71 (2017) 343–358
April

Adsorption of Ni(II) by a polyvinylidene fluoride-type chelating membrane bearing poly(aminophosphonic acid) groups

Xiuli Wang, Laizhou Song*, Feifei Yang, Dandan Yun, Jinbo Wang, Hongye Lu

College of Environmental and Chemical Engineering, Yanshan University, Qinhuangdao 066004, China, Tel. +86 3358387741; Fax: +86 3358061569; emails: songlz@ysu.edu.cn (L. Song), xlwang7904@ysu.edu.cn (X. Wang), Tel. +86 3358061422; Fax: +86 3358061569; emails: yangfeifei2016@126.com (F. Yang), m15232333928@163.com (D. Yun), 532301014@qq.com (J. Wang), 1247867873@qq.com (H. Lu)

Received 28 July 2016; Accepted 10 January 2017

ABSTRACT

A polyvinylidene fluoride (PVDF)-type chelating membrane bearing poly(aminophosphonic acid) groups was fabricated and employed for the removal of Ni(II) from the solution. Effects of pH, initial Ni(II) concentration, temperature and contact time on the Ni(II) adsorption by this membrane were evaluated; also, effects of the coexisting Ca(II), Fe(III), Cd(II), Pb(II), citrate, nitrilotriacetic acid (NTA) and ethylenediaminetetraacetic acid (EDTA) were discussed. The adsorption kinetics and the adsorption isotherms of the membrane toward Ni(II) at the presence of abovementioned seven coexisting specimens were investigated. In addition, the breakthrough curves of the membrane were measured. The presence of coexisting cations and complexing reagents mentioned above reduced the Ni(II) uptake of the membrane. The negative effect of the four cations was in the order of Pb(II) > Cd(II) > Fe(III) > Ca(II); the interference of the three complexing reagents followed the sequence: EDTA > NTA > citrate. The Langmuir and the Lagergren second-order models were excellently competent for the descriptions in adsorption isotherms and adsorption kinetics of the membrane toward Ni(II). The adsorption of Ni(II) by the membrane was a spontaneous and exothermic process.

Keywords: Polyvinylidene fluoride-type chelating membrane; Nickel ion; Adsorption; Coexisting cation; Complexing reagent

1. Introduction

A large volume of wastewater containing Ni(II) has been discharged by the processes, such as mining of nickel ores, metallurgy, manufacturing of circuit board, automobile and aircraft, nickel electroless and electroplating. The nickel ion has been validated as a carcinogen; it can easily accumulate in organisms, and thereby resulting in toxicities to ecological systems and health of human beings [1–3]. The excessive inhalation of nickel and its compounds will lead to hazards of lung diseases and malignant tumors. The discharged concentration of total nickel in China is strictly limited within 0.1 mg/L according to the published Chinese regulation of "Emission standard of pollutants for electroplating (GB 21900-2008)" [4]. Thus, the discharged Ni(II)-containing effluents should be treated to meet the requirement of this legislative standard. In effluents derived from the metallurgy, circuit board manufacture and nickel electroless plating industries, the cations involving Ca(II), Fe(III), Cd(II) and Pb(II), and the organic reagents including citrate, nitrilotriacetic acid (NTA) and ethylenediaminetetraacetic acid (EDTA) can coexist with Ni(II). Undoubtedly, the aforementioned cations and organic reagents coexisting with Ni(II) can hinder the removal of this metal pollutant [5]. Therefore, the exploitation of effective techniques with an excellent disposal performance of Ni(II) is thus of great importance for the removal of this metal ion at the presence of above coexisting substances.

Up to present, numerous techniques including ion exchange, chemical precipitation, biological treatment,

* Corresponding author.

flotation, electrocoagulation, solvent extraction and adsorption process have been employed to remove Ni(II) from wastewater to guarantee this metal pollutant below the limit of discharge standard [6–14]. Of all the abovementioned techniques, adsorption is an efficient and economical treatment process for the removal of Ni(II); especially, this technique is competent for the recycling of Ni(II) from the dilute solution. Consequently, various adsorbents such as activated carbon, lignite, coconut copra meal, fly ash, red mud, kaolinite and montmorillonite, clinoptilolite, chitosan derivative and calcium alginate have been extensively employed for the removal of this metal [15–23].

In contrast with the above processes such as chemical coagulation and precipitation, ion exchange and adsorption, biosorption and electrocoagulation, the membrane separation techniques have exhibited more merits for the disposal of Ni(II), due to the fact of time saving, lower pressure drop and shorter axial-diffusion path [5,24]. Although some powder-type chelating resin adsorbents show a high affinity to Ni(II), the applications of them have been limited because they are not to be easily recovered for reuse. Compared with the adsorption treatment of chelating exchange resins, the membrane technique will be more feasible for the removal of Ni(II) from wastewater because of its advantages of low pressure loss and easy scale-up [25]. As for the membrane techniques of electrodialysis, liquid membrane extraction, polymer-enhanced ultrafiltration, nanofiltration and reverse osmosis, the drawbacks of high costs and fussy pretreatments restrain the wide applications of these membrane techniques [26–30]. The microfiltration and ultrafiltration may be more suitable for removing Ni(II) than the membrane techniques mentioned above, due to the fascinating characteristics of high permeation flux, cost-effective investment and needless strict pretreatments. But, these two conventional membrane techniques cannot remove the dissolvable Ni(II). In light of the adsorption treatment of heavy metals by the chelating resin, the modified microfiltration- or ultrafiltration-type membrane bearing the chelating groups deserves to be exploited for the removal of Ni(II) [5]; the incorporated chelating groups play an important role in the Ni(II) uptake because of their high affinities to this metal ion. Among the chelating groups of polyacrylic acid, pentaethylenehexamine, ethylamine ligand, NTA, polyethyleneimine (PEI), hyperbranched poly(amidoamine) (HPAMAM), EDTA, diethylenetriaminepentaacetic acid (DTPA) and ethylenediamine tetra(methylenephosphonic acid) (EDTMPA), some of them such as PEI, DTPA and HPAMAM groups have attracted enormous attention because of their excellent affinities to metal pollutants [31–33]. The chelating membranes bearing PEI, DTPA and HPAMAM groups have been validated to remove Ni(II) and other metals. However, insufficient investigations have been made focusing on the polyvinylidene fluoride (PVDF) membrane with the incorporation of EDTMPA group for the capture of metals. Hence, the PVDF-based chelating membrane bearing EDTMPA complexing groups employed to remove Ni(II) from the solution, deserves to be investigated.

In this research, a PVDF-type chelating membrane bearing the EDTMPA group was fabricated and employed for the removal of Ni(II) from the aqueous solution. This chelating membrane was characterized using techniques of field emission scanning electron microscope (FE-SEM), energy dispersive X-ray spectrometry (EDS), Fourier transform infrared (FTIR) spectroscopy, X-ray photoelectron spectrum (XPS) and nuclear magnetic resonance (NMR) spectroscopy. Studies regarding the effects of pH, contact time and temperature, initial Ni(II) concentration, flow rate of solution and thickness of membrane stack on the adsorption of Ni(II) by the membrane were conducted. Effects of the coexisting Ca(II), Fe(III), Cd(II) and Pb(II), as well as the complexing reagents including citrate, NTA and EDTA on the uptake of Ni(II) were also studied. The batch adsorption experiments with respect to the kinetics and isotherms were performed with the presence of the abovementioned cations and complexing reagents. In addition, the breakthrough curves of the chelating membrane were determined by continuous adsorption tests. Lastly, the reused property of this membrane was evaluated.

2. Materials and methods

2.1. Materials

The molecular weight of PVDF powders provided by Chen Guang Co., Ltd. (Chengdu, China) was ca. 400,000. Analytical grade polyvinylpyrrolidone (PVP) as pore-forming additive, dimethyl sulfoxide (DMSO) as solvent, EDTMPA and tetrabutyl orthotitanate (TBOT) were applied for the preparation of the chelating group of the membrane. Analytical grade reagents of $Ni(NO_3)_2{\cdot}6H_2O$, $Pb(NO_3)_2$, $Cd(NO_3)_2{\cdot}4H_2O$, $CaCl_2{\cdot}4H_2O$, $Fe_2(SO_4)_3{\cdot}4H_2O$, NaOH, H_2SO_4 (98 wt%), citrate, NTA, ethylenediaminetetraacetic acid disodium salt (EDTA-$2Na^+$), absolute ethanol, sodium acetate and glacial acetic acid were supplied by Jingchun Scientific Co., Ltd. (Shanghai, China) and used as received. A stock Ni(II) solution with a concentration of 17 mmol/L was prepared by dissolving weighed amounts of $Ni(NO_3)_2{\cdot}6H_2O$ in deionized water. The working solutions containing Ni(II) were prepared by diluting the stock solution to appropriate volumes. The concentrations of stock solutions containing the coexisting cation and organic acid were 0.1 and 0.2 mol/L, respectively.

2.2. Preparation of the PVDF-based chelating membrane

The schematic preparation process of the chelating membrane was displayed in Fig. 1. First, 2.0 g of EDTMPA was dissolved in 40 mL of ethanolaqueous solution (volume ratio between C_2H_5OH and H_2O was 1:3), and pH of the solution was adjusted to 6.0 by 5 mol/L of NaOH solution. Then, 4.7 mL of TBOT was added dropwise into this solution; this solution was magnetically stirred for 24 h at room temperature, and a soliquoid was obtained. After that, the soliquoid was centrifugally separated at a rate of 3,000 rpm for 10 min, the obtained powder (denoted as EDTMPA–TBOT) was centrifugally washed three times using absolute ethanol and DMSO. Afterward, 4.8 g of PVDF and 0.53 g of PVP were dissolved in 25 mL of DMSO at 353 K, followed the addition of all above fabricated EDTMPA–TBOT powder, and then the solution was stirred for 6 h at this temperature. Lastly, the PVDF-based chelating membrane was prepared via a phase inversion technique with deionized water employed as the coagulation bath. The obtained membrane (EDTMPA–TBOT/PVDF) was cleaned with deionized water and kept for subsequent characterization and adsorption experiments.

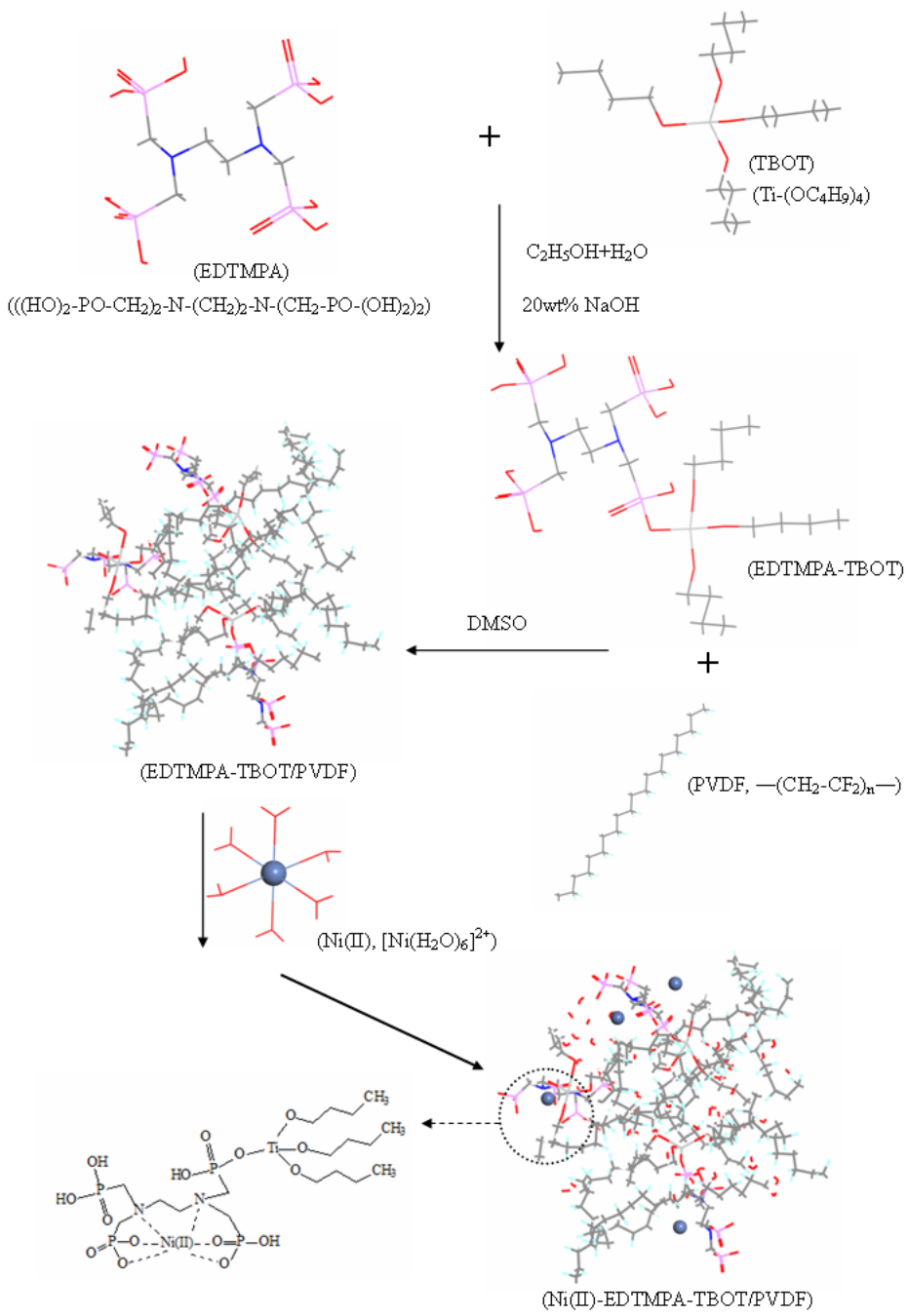

Fig. 1. Schematic diagram of the EDTMPA–TBOT/PVDF membrane preparation process and the Ni(II) adsorption.

2.3. Membrane characterization

A FE-SEM (SUPRA55, Zeiss, Germany) with an accelerating voltage of 5 kV was employed to characterize the morphology of the chelating membrane; compositions of the surface membrane were determined by the EDS (X-Max, Oxford Instruments, UK) attached to this scanning microscope. An E55+FRA106 FTIR spectrometer (Bruker, Germany) was adopted to examine the FTIR spectra of EDTMPA–TBOT chelating group before and after the adsorption of Ni(II). The elements on the chelating membrane after the Ni(II) uptake were measured by an XPS spectrometer (ESCALAB 250, Thermo Fisher, UK) with Al Kα as the excitation source; the C 1s peak from graphitic carbon at 284.6 eV was employed to calibrate the binding energy. The chemical groups of the chelating membrane before and after the uptake of Ni(II) were characterized with a solid-NMR spectrometer (BRUKER AVANCE III 400, Karlsruhe, Germany). In addition, the mean pore size of the chelating membrane was characterized by water permeability method [34]; the point of zero charge (pH_{pzc}) of the chelating membrane was determined using a batch equilibration method [35].

2.4. Adsorption experiments

Batch adsorption experiments were conducted in 200 mL of Ni(II) solutions with ~0.2 g addition of the chelating membrane [36]. The effect of pH was investigated and pH values were adjusted to 1.0–7.5 using 0.3 mol/L acetic acid and 0.2 mol/L sodium acetate buffer, and 0.2 mol/L sodium hydroxide solution. The determined optimal pH from this test was adopted for all experiments. Effects of the contact time (0–480 min), temperature (288, 298 and 308 K) and the initial Ni(II) concentration (0.34–2.0 mmol/L) were also evaluated. For each test, 1 mL of aliquot was withdrawn from the working solution to determine the residual Ni(II) concentration at different time intervals (i.e., 5, 10, 30 and 60 min) till equilibrium by an atomic absorption spectrophotometer (AA6800, Shimadzu, Japan). The amounts of Ni(II) adsorbed on the chelating membrane were calculated as follows [5,37]:

$$q_t = \frac{(c_0 - c_t) \times V}{M} \times 58.7 \quad (1)$$

where q_t is the Ni(II) uptake of a unit weight of the membrane (mg/g) at time t. c_0 and c_t are the concentrations of Ni(II) at initial and time t in the aqueous phase (mmol/L), respectively. V is the volume of the aqueous phase (L), M is the dry weight of the chelating membrane (g) and 58.7 is the molar mass of Ni(II) (g/mol). The effects of coexisting Ca(II), Fe(III), Cd(II), Pb(II), citrate, NTA and EDTA on the Ni(II) uptakes were evaluated at 298 K as similar to the process of single Ni(II) system; solutions containing 1.0 mmol/L of Ni(II) with different concentration of the abovementioned cations and complexing reagents (0–5 mmol/L).

Adsorption kinetics was investigated in solutions containing 1.0 mmol/L Ni(II) at 298 K. The adsorption kinetics with the presence of Ca(II), Fe(III), Cd(II), Pb(II), citrate, NTA and EDTA were also studied; concentrations of these seven coexisting specimens were 1 mmol/L. Adsorption isotherms were examined in 0.34–2.0 mmol/L Ni(II) solutions with the addition of the above coexisting specimens (1 mmol/L) at 298 K. The initial and equilibrium concentrations of Ni(II) were measured. Each experiment was performed in triplicate to guarantee the accuracy of experimental data, and the average value was recorded.

The continuous adsorption experiments were carried out in a single-pass mode, the Ni(II)-containing solutions were circulated at three different flow rates (i.e., 0.062, 0.128 and 0.166 cm/min) using a peristaltic pump (BT00-300M, Longer Pump Co. Ltd., Baoding, China) through a membrane stack. The detailed setup of the membrane stack was previously described [38], where the membranes with a thickness of 267 μm were sealed layer by layer into an ultrafiltration cup with an inner diameter of 75 mm (YL-300, Yuling Filtering Instrument Co. Ltd., Shanghai, China). Three membrane stacks consisting of three, four and five flat-sheeted membranes were structured; the total thicknesses of them were 0.8, 1.07 and 1.34 mm. The membrane stacks were placed in a water-jacketed thermostatic incubator (GHP-80, Birgit Experimental Instrument Factory, Jintan, China). The solution in the ultrafiltration cup was stirred by a magnetic stirrer (HJ-5, Huanxi Medical Instrument Co. Ltd., Shanghai, China). The concentration of Ni(II) at the outlet was measured at different time intervals (i.e., 10 and 30 min). Thus, the breakthrough curves of the single Ni(II) system, and those of systems with the presence of Ca(II), Fe(III), Cd(II), Pb(II), citrate, NTA and EDTA were obtained. During these tests, the transmembrane pressure (TMP), i.e., the difference between the inlet pressure and the outlet pressure was also measured.

Breakthrough curves were analyzed by the model of bed depth service time (BDST) proposed by Bohart and Adams [39], which was described via Eq. (2) [40,41]. This model can be employed to predict the relationship between the thickness of membrane stack (Z) and breakthrough time (t_b, the time as the Ni(II) concentration in effluent vs. its initial concentration is 0.05):

$$t_b = \frac{N_0}{c_0 v} Z - \frac{1}{K_a c_0} \ln\left(\frac{c_0}{c_b} - 1\right) \quad (2)$$

where N_0 is the sorption capacity of membrane stack (mmol/L), v is the influent linear velocity (cm/min), c_0 and c_b (mmol/L) are the concentrations of Ni(II) in influent and in effluent at time t_b, respectively. K_a is the rate constant in the BDST model (L/min mmol), representing the transferring rate of Ni(II) from the solution to the chelating membrane.

2.5. Adsorption/desorption experiment

A 0.5 mol/L of H_2SO_4 solution as the elution agent was employed to evaluate the desorption efficiency of the chelating membrane. In the static desorption test, the membrane loading Ni(II) with a dry weight of ~0.2 g was immersed in 200 mL of H_2SO_4 solution. After the adsorbed Ni(II) was eluted from the surface of membrane, the chelating membrane was again immersed into 1.0 mmol/L of Ni(II) solution for the capture of Ni(II). The adsorption/desorption processes for the same membrane were repeated 10 times. The amounts of Ni(II) adsorbed and eluted during the adsorption/desorption processes were determined. The desorption efficiency (DE) was evaluated using Eq. (3) [37]:

$$DE = (q_1 / q_0) \times 100\% \quad (3)$$

where q_1 is the desorbed amount of Ni(II) from the membrane (mg/g) and q_0 is the adsorbed amount of Ni(II) on the membrane at equilibrium (mg/g).

3. Results and discussion

3.1. Characterization of the chelating membrane

3.1.1. FE-SEM and EDS analyses

The surface and sectional morphologies of the EDTMPA–TBOT/PVDF chelating membrane are displayed in Fig. 2. As indicated by the surface morphology (Fig. 2(a)), the chelating membrane exhibits a uniform microporous structure. The determined average size of the micropore is 0.25 μm, and thereby suitable for the permeation of solutions through this membrane. As shown in Fig. 2(b), the finger-like pores (labeled by a rectangle) can be found near the surface layer

of the membrane, and the sponge-shaped porous structures (described by a circle) are observed in the inner side of the membrane.

EDS spectra of the chelating membrane before and after Ni(II) adsorption were examined (Figs. 2(c) and (d)). The weight contents (wt%) of elements on the surface of the membrane obtained by the ZAF normalization are tabulated in Table 1. After the uptake of Ni(II), besides elements of carbon, nitrogen, oxygen, fluorine, phosphorus and titanium, the nickel element is also detected, illustrating the Ni(II) adsorption by the EDTMPA–TBOT/PVDF chelating membrane.

3.1.2. FTIR spectra

The availability of EDTMPA–TBOT/PVDF chelating membrane toward Ni(II) was validated by FTIR analysis (Fig. 3). Compared with that of the virgin PVDF membrane, the peaks of appearing at 890–1,400 cm^{-1} (Fig. 3(a)) changed obviously due to the incorporation of EDTMPA–TBOT powder and the existence the phosphonic acid groups. However, for the chelating membrane before and after Ni(II) adsorption, the difference in FTIR spectra is unconspicuous because of the disturbance of PVDF chains. Therefore, in order to eliminate this disturbance, FTIR spectra of the virgin EDTMPA and the EDTMPA–TBOT powder before and after Ni(II) adsorption were also measured, and the spectra are shown in Fig. 3(b). The peaks appearing at 957 and 1,007 cm^{-1} are ascribed to the asymmetric stretching vibration of P–OH groups, and the peaks locating at 1,100–1,270 cm^{-1} are attributed to P=O stretching vibration [42,43]. The peaks at 1,322 and 1,435 cm^{-1} can be assigned to the stretching vibration of C–N and P–C groups, respectively; the broad peak at 1,670 cm^{-1} can be identified to the plane bending of hydroxyl group in phosphonic acid group [44]. For the spectrum of EDTMPA–TBOT sample, it can be observed that the characteristic peaks of phosphonic acid group (in the range of 900–1,270 cm^{-1} range) change into two peaks centered at 1,030 and 1,150 cm^{-1}, which could be attributed to the formation of P–O–Ti bond [45]; the broad peak at 1,670 cm^{-1} becomes sharply and shifts to 1,650 cm^{-1}. This indicates the interaction between TBOT and EDTMPA molecules, and thereby suggesting the formation of P–O–Ti bond. After the Ni(II) adsorption, in comparison with that before the Ni(II)

Table 1
The element weight content (wt%) of chelating membrane determined by EDS before and after Ni(II) adsorption

Element (wt%)	C	N	O	F	P	Ti	Ni
Before Ni(II) adsorption	34.90	1.16	9.91	50.21	2.80	1.02	–
After Ni(II) adsorption	34.45	1.38	8.37	51.39	2.45	0.95	1.01

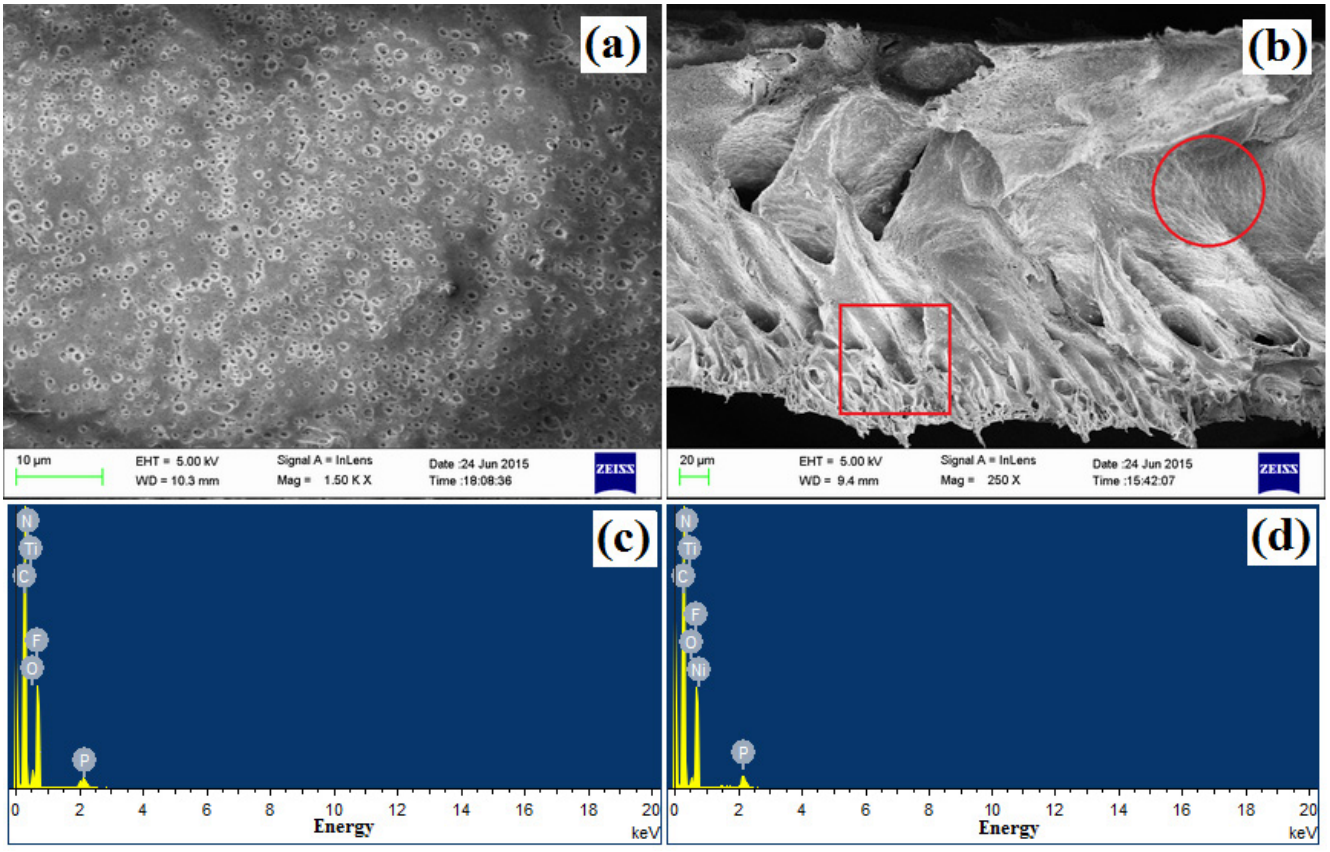

Fig. 2. FE-SEM pictures and EDS spectra of the EDTMPA–TBOT/PVDF membrane: (a) surface morphology; (b) sectional morphology; (c) EDS before Ni(II) adsorption and (d) EDS after Ni(II) adsorption.

adsorption, the peak at 1,030 cm^{-1} shifts to 1,047 cm^{-1} and the intensity of this peak also slightly increases. The intensity of peak at 1,150 cm^{-1} related to P=O stretching decreases, which can be assigned to the formation of P=O–Ni(II) complexing bond. The peak at 1,322 cm^{-1} in correlation with the C–N group almost completely disappears, thus indicating the formation of the N–Ni(II) bond [37]. Also, the decreasing intensity of the peak at 1,650 cm^{-1} and the negative shift of 15 cm^{-1} may be due to the complexing interaction between Ni(II) and O–H in phosphonic acid groups [5,46].

3.1.3. XPS analysis

For the purpose of further elucidating the adsorption characteristic of the chelating membrane toward Ni(II), XPS measurement was performed (Fig. 4). Considering the fact that the Ni 2p signal was intensively interfered by the Auger signal of fluorine element of PVDF, both the XPS spectrum of EDTMPA–TBOT/PVDF chelating membrane before the adsorption of Ni(II) and that of EDTMPA–TBOT powder after the Ni(II) uptake were measured. As for the XPS spectrum of EDTMPA–TBOT/PVDF chelating membrane (Fig. 4(a)), in addition to the characteristic peaks of C 1s (286.3 eV) and F 1s (688.3 eV) for the PVDF polymer chain, peaks at 132.9 eV for P 2p (inset (1)), 400.3 eV for N 1s, O 1s (532.3 eV) and 463.1 eV for Ti 2p (inset (2)) are clearly observed, which indicates that the EDTMPA–TBOT chelating group was successively incorporated into the PVDF matrix. For the spectrum of EDTMPA–TBOT powder after Ni(II) adsorption (Fig. 4(b)), peaks appearing at 133.3, 285.3, 400.3, 459.3 and 531.3 eV are

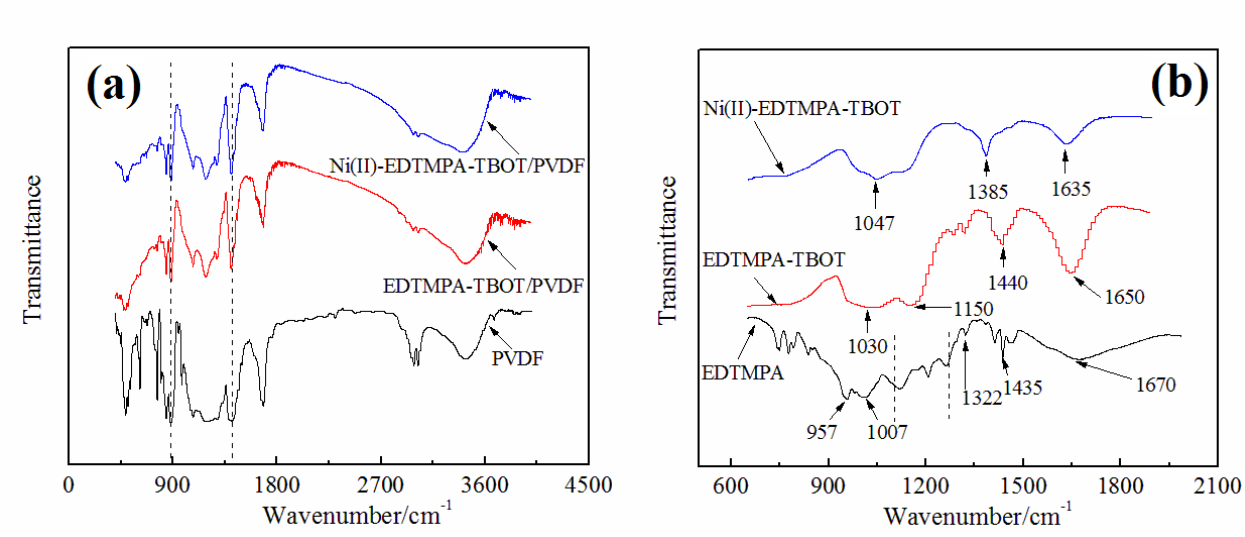

Fig. 3. FTIR spectra: (a) the virgin PVDF membrane and the EDTMPA–TBOT/PVDF chelating membrane before and after Ni(II) adsorption and (b) the virgin EDTMPA and the EDTMPA–TBOT powder before and after Ni(II) adsorption.

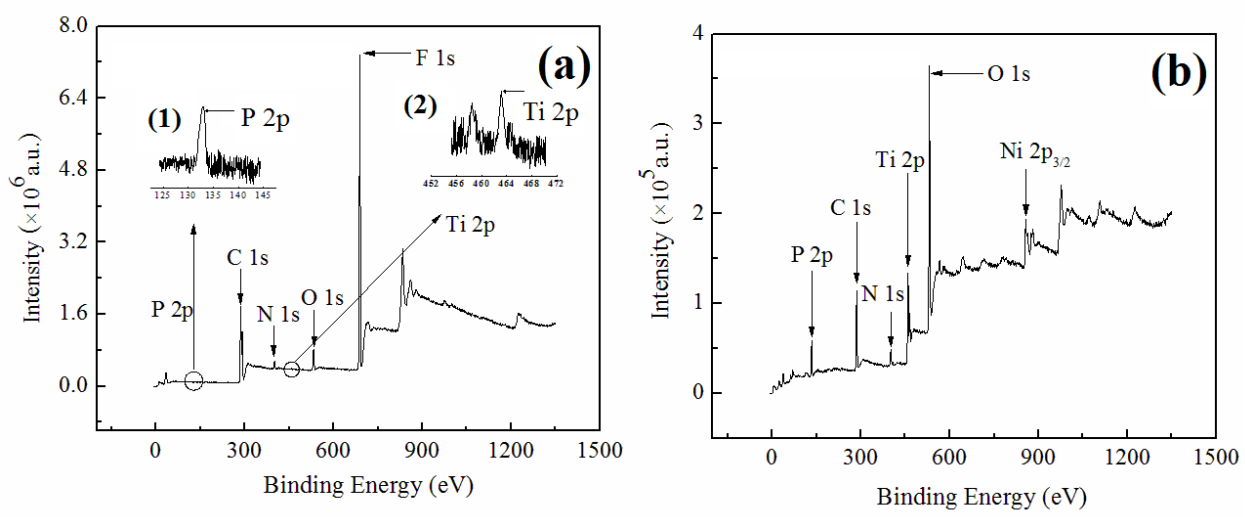

Fig. 4. XPS spectra: (a) the EDTMPA–TBOT/PVDF chelating membrane before Ni(II) adsorption and (b) the EDTMPA–TBOT power after Ni(II) adsorption.

identified to P 2p, C 1s, N 1s, Ti 2p and O 1s, respectively. The new peak at 857.3 eV can be attributed to Ni $2p_{3/2}$ [47], suggesting that Ni(II) is complexed by the EDTMPA–TBOT chelating ligand.

3.1.4. NMR analysis

The ^{13}C and ^{31}P solid-state NMR spectra of the chelating membrane before and after Ni(II) adsorption were measured, and the tested spectra are shown in Fig. 5. As shown in the ^{13}C NMR spectrum (Fig. 5(a)), the peaks at 43.1 and 120.0 ppm can be attributed to the $–CH_2–$ and $–CF_2–$ groups of the PVDF chain [5,48]; peaks appearing at 18.9 and 31.0 ppm are indexed to $–CH_3$ and $–CH_2–$ groups of TBOT; the peak at 176.4 ppm is assigned to the acylamide groups of the residual PVP (the pore-forming additive) [49]. The two peaks appearing at 52.9 and 70.0 ppm can be assigned to $–CH_2N–$ group and $–CH_2–P$ group of EDTMPA molecule [50,51]. After Ni(II) adsorption, the disappearance of peak at 52.9 ppm and the intensity decrease of peak at 70.0 ppm indicate that the nitrogen atoms of $–CH_2N–$ groups and oxygen atoms of phosphonic acid groups are chelated by Ni(II) [37,49]. In addition, as to the ^{31}P NMR spectrum (Fig. 5(b)), two signals of the chelating membrane before Ni(II) adsorption at 6.6 and 17.9 ppm are detected, corresponding to P_1, P_3, P_4 and P_2 atoms of EDTMPA–TBOT group (molecular structure in inset (b)-1) [52]. After Ni(II) adsorption, the peak at 6.6 ppm was divided into two peaks (appearing at 5.3 and 7.7 ppm), which can be assigned to P_1, and P_3 and P_4 (molecular structure in inset (b)-2). Also, the peak at 17.9 ppm shifts to 16.9 ppm and the intensity of this peak decreases. These results can be ascribed to the chelation between Ni(II) and EDTMPA–TBOT group, and thus resulting the chemical shifts of P_3 and P_4 atoms to a low field, while those of P_1 and P_2 atoms to a high field. Therefore, we confirm that the EDTMPA–TBOT/PVDF chelating membrane is competent for the capture of Ni(II), so achieving the removal of this metal from aqueous solutions.

3.2. Effects of pH, contact time, initial Ni(II) concentration, temperature and flow rate

3.2.1. Effect of pH

The influence of pH on the Ni(II) uptake of the chelating membrane is shown in Fig. 6(a). The Ni(II) uptake of the chelating membrane is strongly dependent on the variation of pH; it increases when pH rises from 1.0 to 5.4, then it

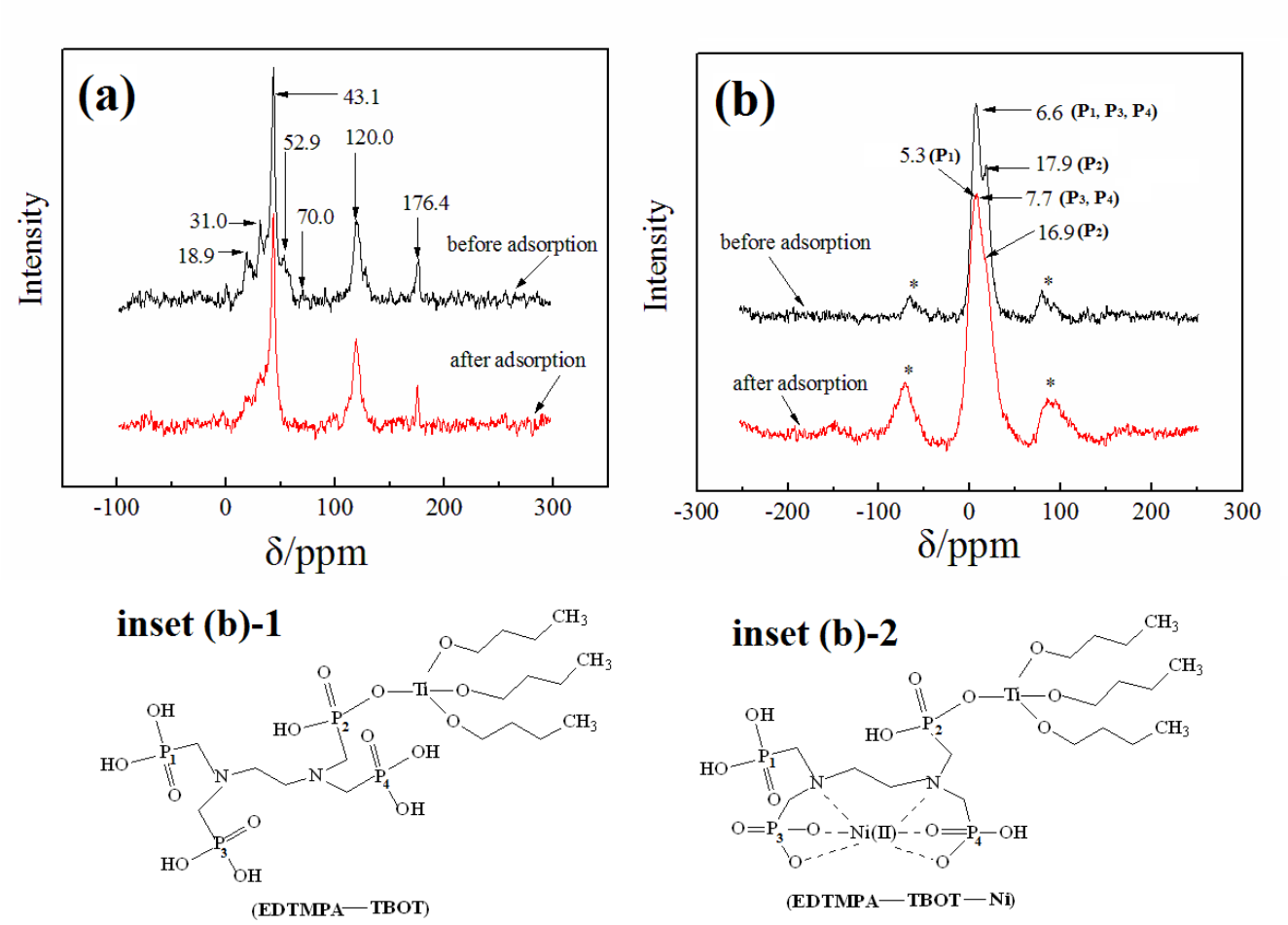

Fig. 5. Solid-state NMR spectra: (a) ^{13}C NMR of the EDTMPA–TBOT/PVDF membrane before and after Ni(II) adsorption and (b) ^{31}P NMR of the EDTMPA–TBOT/PVDF membrane before and after Ni(II) adsorption.

decreases with the increase in pH value, and the optimal pH is 5.4. The determined pH_{pzc} of the chelating membrane is 5.4, consistent with the optimal pH value. At low pH values, the N atoms of EDTMPA–TBOT group are protonated and the competition between H^+ and Ni(II) do not favor the chelating process due to the electrostatic repulsion. Whereas, as pH increases, the adsorption process of Ni(II) tends to occur with the deprotonated complexing groups, thereby resulting in the enhancement in the Ni(II) uptake. Herein, the optimum pH of 5.4 was adopted for all the following experiments.

3.2.2. Effect of contact time

The Ni(II) uptakes of the chelating membrane as a function of time at different temperatures are presented in Fig. 6(b). As shown by Fig. 6(b), the time required to achieve equilibrium for Ni(II) uptake is 360 min. Two stages including rapid and slow stage can be observed in the adsorption process. The rapid stage occurs within the first 120 min, while the slow adsorption extends for the remaining 240 min. At the beginning of the adsorption process, there are plentiful spare adsorption sites on the surface of the membrane, which will be of benefit for the uptake of Ni(II). After 120 min, the consumption of adsorption sites will reduce the adsorption of Ni(II). In addition, as the temperature increases, the adsorption capacity of the membrane toward Ni(II) decreases. Hence, it can be inferred that the Ni(II) adsorption is an exothermic process.

3.2.3. Effects of initial Ni(II) concentration and temperature

The Ni(II) adsorption on the chelating membrane varying with the change in the initial Ni(II) concentration at different temperature is presented in Fig. 6(c). As the initial concentration of Ni(II) varies from 0.34 to 2.0 mmol/L, the Ni(II) uptake at 298 K increases from 18.6 to 29.6 mg/g. However, the removal efficiency of Ni(II) decreases from 98% to 25%. The descending trend in the Ni(II) uptake at the three temperatures follows the order of 288 K > 298 K > 308 K (Fig. 6(c)), indicating the exothermic nature of this adsorption process. Thus, the low values in Ni(II) concentration and temperature will be helpful in the capture of Ni(II).

3.2.4. Effect of flow rate

The effect of the flow rate on the Ni(II) uptake of the membrane is reported in Fig. 6(d). When the flow rate increases from 0.062 to 0.128 and 0.166 cm/min, the Ni(II) uptake reduces from 29.8 to 28.6 and 27.6 mg/g, corresponding to a decrease of 4% and 7%, respectively. The high flow rate will shorten the adsorption time, thereby reducing the Ni(II) uptake of the membrane. Thus, a low flow rate will be favor to the adsorption [38]; herein, the flow rate of 0.128 cm/min was adopted for the following tests. In addition, the equilibrium time for the Ni(II) adsorption is postponed when the thickness of membrane stack increases from 0.8 to 1.07 and 1.34 mm (Fig. 6(e)); however, the change in the Ni(II) uptake at equilibrium is unremarkable.

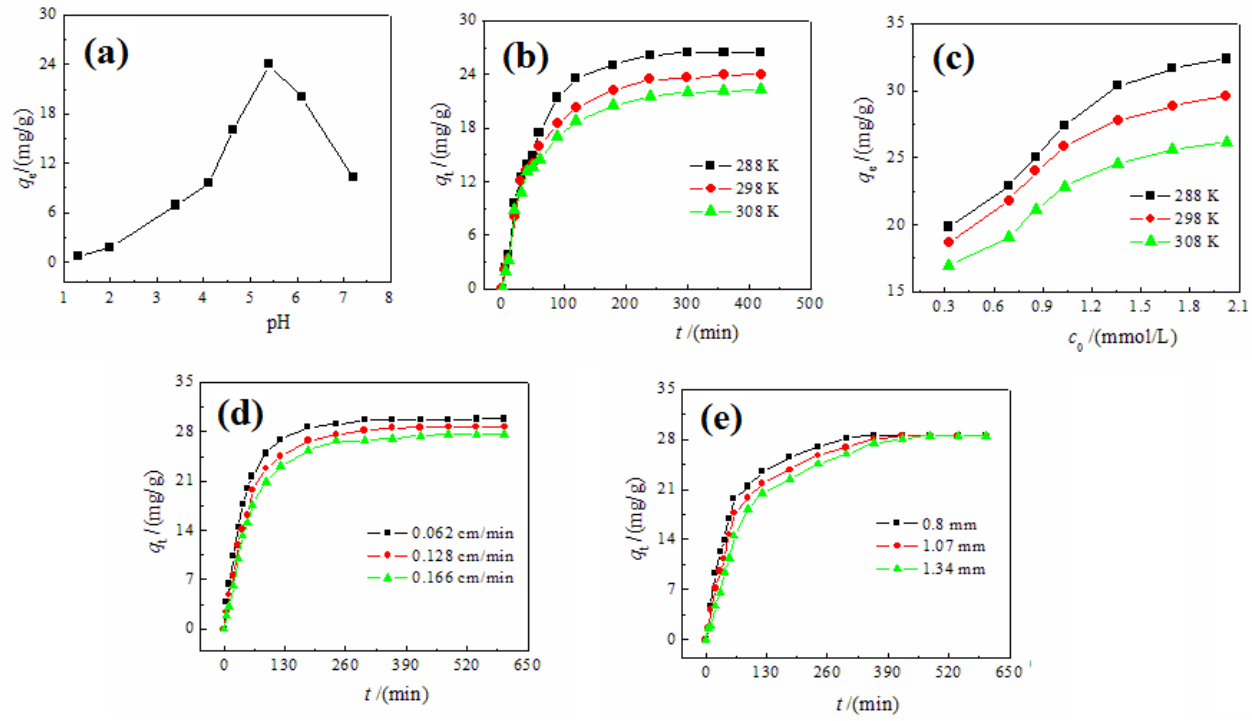

Fig. 6. Effects of pH, contact time and temperature, initial Ni(II) concentration, flow rate, thickness of membrane stack on Ni(II) adsorption: (a) pH (c_0(Ni(II)) = 1.0 mmol/L; t: 360 min; membrane addition: ~0.2 g; T: 298 K); (b) contact time and temperature (c_0(Ni(II)) = 1.0 mmol/L; membrane addition: ~0.2 g; pH: 5.4); (c) initial Ni(II) concentration (t: 360 min; membrane addition: ~0.2 g; T: 298 K; pH: 5.4); (d) flow rate (c_0(Ni(II)) = 1.0 mmol/L; thickness of membrane stack: 0.8 mm; T: 298 K; pH: 5.4) and (e) thickness of membrane stack (c_0(Ni(II)) = 1.0 mmol/L; flow rate: 0.128 cm/min; T: 298 K; pH: 5.4).

3.3. Effects of coexisting cations and complexing reagents

The coexisting cations involving Ca(II), Fe(III), Cd(II) and Pb(II), and the coexistent complexing reagents including citrate, NTA and EDTA can hinder the Ni(II) adsorption. Ni(II) uptakes of the EDTMPA–TBOT/PVDF membrane at the presence of the above seven specimens were measured to elucidate the interferences of them. Ni(II) uptakes of the membrane reduce with the increase in concentrations of Ca(II), Fe(III), Cd(II) and Pb(II) from 0 to 5 mmol/L (Fig. 7(a)), these four coexisting cations shows a negative effect on the Ni(II) adsorption because they compete with Ni(II) for occupying the active sites. When the concentration of Ca(II), Fe(III), Cd(II) and Pb(II) is 1 mmol/L, Ni(II) uptake of the membrane decreases by 35%, 45%, 65% and 83%. Based on this result, it can be inferred that the chelating membrane exhibits a more excellent affinity to Pb(II), Cd(II) and Ni(II) than Fe(III) and Ca(II), so EDTMPA–TBOT/PVDF membrane will be competent for the removal of heavy metals with a high biotoxicity. The detrimental effect of these four cations follows the order: Pb(II) > Cd(II) > Fe(III) > Ca(II); thus it can be deduced that the affinity of the membrane to these four coexisting cations is in the sequence of Ca(II) < Fe(III) < Cd(II) < Pb(II).

The influences of citrate, NTA and EDTA with different concentrations on Ni(II) uptakes of the chelating membrane are shown in Fig. 7(b). As the concentration of the three complexing reagents increase from 0 to 5 mmol/L, the Ni(II) uptake of the chelating membrane decreases. This can be explained that most nickel ions are complexed with the increasing concentration of these complexing reagents, and the complexed form of Ni(II) retards this metal uptake to some extent. As citrate, NTA and EDTA coexisted at the concentration of 1 mmol/L, the Ni(II) uptake of the membrane decreases by 26%, 53% and 73%, respectively. Thus, it can be concluded that the interference of the three complexing reagents is in the order of citrate < NTA < EDTA. In spite of the disturbances of coexisting cations and complexing reagents, the chelating membrane still exhibits the ability of Ni(II) adsorption, manifesting its potential application in the removal of Ni(II) from aqueous solutions.

The Ni(II) uptakes of some reported adsorbents are tabulated in Table 2. By comparison of the reported Ni(II) uptakes [12,17,20,23,53,54], the fabricated EDTMPA–TBOT/PVDF chelating membrane shows an excellent performance in the

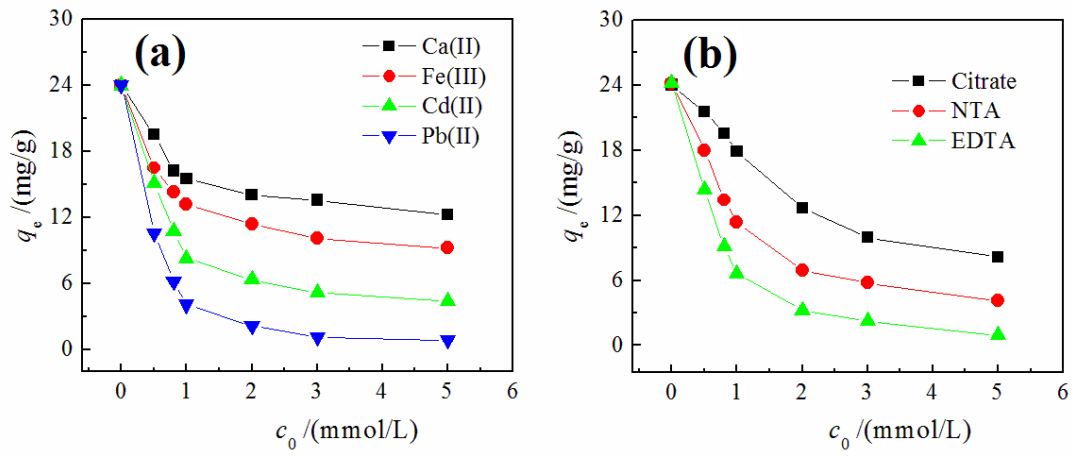

Fig. 7. Effects of concentrations for the coexistent cations and complexing reagents on Ni(II) adsorption: (a) coexistent cations and (b) complexing reagents. c_0(Ni(II)) = 1.0 mmol/L; t: 360 min; membrane amount: ~0.2 g; T: 298 K; pH: 5.4.

Table 2
Comparison in Ni(II) uptake of different adsorbents

Adsorbent	Test condition					Ni(II) uptake (mg/g)	Refs.
	pH	Ni(II) concentration (mmol/L)	Temperature (K)	Time (h)	Adsorbent addition (g/L)		
EDTMPA–TBOT/PVDF chelating membrane	5.4	1.0	298	6	1	24.0	This test
Irish peat moss	4.5	1.70	298	24	4	15.0	[12]
Coconut copra meal	5.0	1.0	299	2	20	1.7	[17]
Montmorillonite	5.7	0.85	303	3	2	12.7	[20]
Kaolinite						5.2	
Calcium alginate	5.0	1.70	Room temperature	1.5	1.5	62.0	[23]
Sulphuric acid-treated Parthenium carbon	5.0	0.43	296	4	2	9.47	[53]
Red mud	5.0	0.43	303	4	10	2.24	[54]

adsorption of Ni(II). Except for the high affinity to Ni(II), the EDTMPA–TBOT/PVDF membrane also shows the excellent capture behavior of Cd(II) and Pb(II). From this point of view, we confirm that this fabricated chelating membrane will be applicable for the removal of metals with a high toxicity from the aqueous solution.

3.4. Studies of adsorption kinetics and adsorption isotherm

In order to evaluate the adsorption characteristic of the EDTMPA–TBOT/PVDF chelating membrane toward Ni(II), the adsorption kinetics and adsorption isotherm of the chelating membrane toward Ni(II) in eight systems: single Ni(II), Ni(II)–Ca(II), Ni(II)–Fe(III), Ni(II)–Cd(II), Ni(II)–Pb(II), Ni(II)–citrate, Ni(II)–NTA and Ni(II)–EDTA were investigated. The experimental kinetics data for abovementioned systems were described in Fig. 8 and analyzed by Lagergren first-order and Lagergren second-order equations [17,20]. The analyzed parameters are reported in Table 3, where q_{et} (mg/g) is the amount of adsorbed Ni(II) at equilibrium; and k_1 (1/min) and k_2 (g/(mg min)) are the rate constants of these two kinetic equations. Compared with the single Ni(II) system, the coexisting cations (Ca(II), Fe(III), Cd(II) and Pb(II)) and complexing reagents (citrate, NTA and EDTA) results in the decrease in Ni(II) uptake of the membrane (Figs. 8(a) and (b)), showing the disturbances of them. The disturbance of these four cations follows the sequence: Pb(II) > Cd(II) > Fe(III) > Ca(II). As indicated by Table 3, the Lagergren second-order adsorption model is more suitable than the Lagergren first-order model for describing the adsorption kinetics of the membrane toward Ni(II) because of the higher coefficient of determination ($R^2 > 0.99$). Therefore, in the adsorption process of Ni(II), the chemisorption may play a more important role than physisorption [37]. By the comparison of k_2, it can be concluded that the competitive adsorption between Ni(II) and the four coexisting cations accelerates the sorption process,

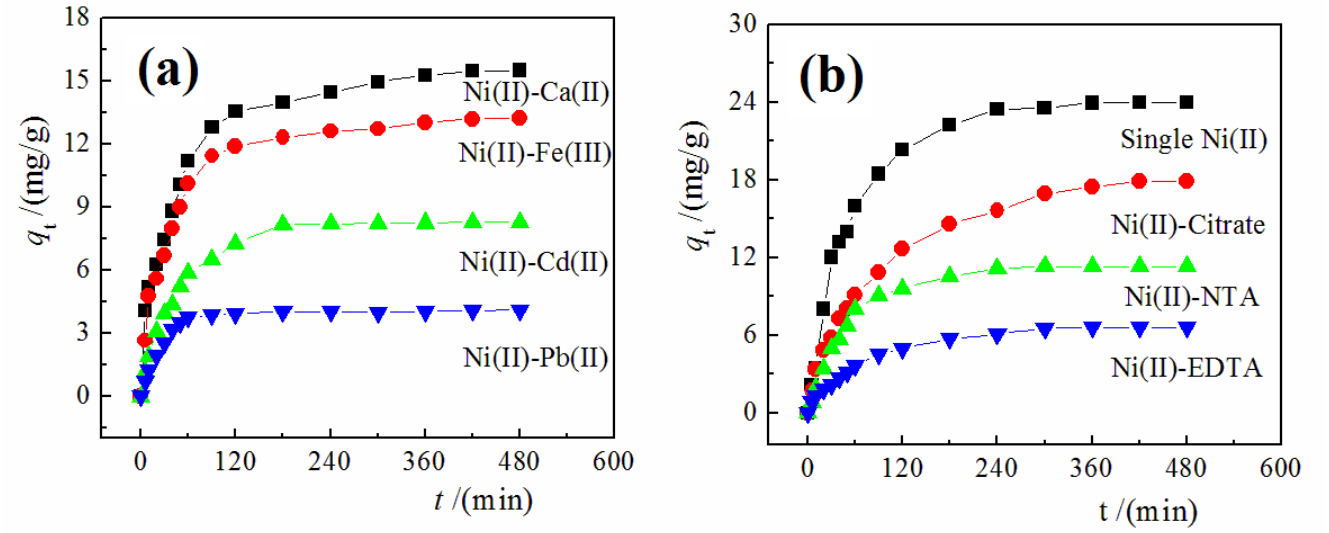

Fig. 8. Adsorption kinetics for Ni(II) onto the EDTMPA–TBOT/PVDF membrane: (a) the cation coexisting systems and (b) the complexing reagent coexisting systems. c_0(Ni(II)) = c_0(Ca(II)) = c_0(Fe(III)) = c_0(Cd(II)) = c_0(Pb(II)) = c_0(citrate) = c_0(NTA) = c_0(EDTA) = 1.0 mmol/L; T: 298 K; pH: 5.4; membrane addition: ~0.2 g.

Table 3
Adsorption parameters of Lagergren first-order and Lagergren second-order models for the chelating membrane toward Ni(II) at 298 K

System	Lagergren first-order model $\ln(q_e - q_t) = \ln q_{et} - k_1 t$			Lagergren second-order model $\frac{t}{q_t} = \frac{1}{k_2 q_{et}^2} + \frac{t}{q_{et}}$		
	k_1 (1/min)	q_{et} (mg/g)	R^2	k_2 (×10^{-3} g/(mg min))	q_{et} (mg/g)	R^2
Single Ni(II)	0.0173	22.12	0.982	0.824	26.83	0.996
Ni(II)–Ca(II)	0.0135	10.36	0.983	2.166	16.39	0.998
Ni(II)–Fe(III)	0.0126	8.05	0.967	2.879	13.92	0.999
Ni(II)–Cd(II)	0.0111	6.68	0.973	3.233	9.05	0.998
Ni(II)–Pb(II)	0.0091	3.41	0.987	3.448	4.26	0.998
Ni(II)–citrate	0.0156	16.59	0.989	1.338	20.61	0.997
Ni(II)–NTA	0.0121	11.21	0.989	1.653	12.79	0.995
Ni(II)–EDTA	0.0106	5.93	0.994	2.205	7.57	0.995

due to the large values of k_2 for Ni(II)–Ca(II), Ni(II)–Fe(III), Ni(II)–Cd(II), Ni(II)–Pb(II) systems; similar results for the three complexing reagent-containing systems can also be attested. In addition, for the three complexing reagent coexisting systems, the value of q_{et} follows the sequence of single Ni(II) > Ni(II)–citrate > Ni(II)–NTA > Ni(II)–EDTA, indicating the interference of those three complexing reagents on the Ni(II) uptake. The negative effect of EDTA is much higher than those of other two complexing reagents.

The thermodynamic behaviors of the chelating membrane toward Ni(II) in the single Ni(II), and the seven cations and complexing reagent coexisting systems are interpreted by Freundlich, Langmuir and Dubinin–Radushkevich (D–R) isotherm models [55,56]. The isotherm experimental data of the single Ni(II), four cations and three complexing reagents coexisting systems are shown in Figs. 9(a) and (b).

The analyzed parameters of the abovementioned three models are listed in Table 4, where q_e (mg/g) is the amount of Ni(II) adsorbed at equilibrium, q_m (mg/g) is the maximum adsorption capacity of the membrane. K_F and $1/n$ are the Freundlich constants related to the adsorption capacity and the adsorption intensity; b (L/mg) is the Langmuir adsorption constant. E (kJ/mol) is the mean free energy of adsorption. In view of the determination coefficients (R^2), the Langmuir isotherm model (R^2 > 0.99) is more competent than Freundlich and D–R models for the description in the thermodynamic behavior of the Ni(II) uptake. As demonstrated by the data (Table 4), the value of q_m at 298 K derived from the Langmuir model is slightly greater than the experimental value because of some adsorption sites of the membrane are unoccupied. The Langmuir parameter b associated with the adsorption affinity for the above

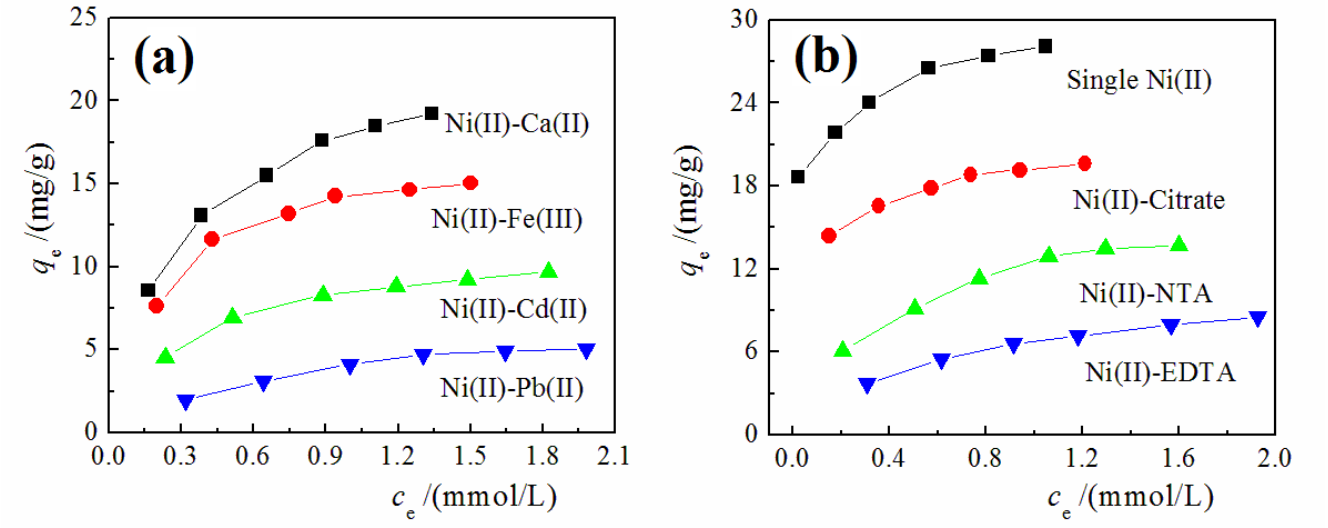

Fig. 9. Adsorption isotherm for Ni(II) onto the EDTMPA–TBOT/PVDF membrane: (a) the cation coexisting systems and (b) the complexing reagent coexisting systems. c_0(Ca(II)) = c_0(Fe(III)) = c_0(Cd(II)) = c_0(Pb(II)) = c_0(citrate) = c_0(NTA) = c_0(EDTA) = 1.0 mmol/L; t: 360 min; T: 298 K; pH: 5.4; membrane addition: ~0.2 g.

Table 4
Adsorption parameters of Langmuir, Freundlich and D–R models for the chelating membrane toward Ni(II) at 298 K

System	Freundlich model $\lg q_e = \lg k_F + \frac{1}{n}\lg c_e$			Langmuir model $\frac{c_e}{q_e} = \frac{1}{q_m b} + \frac{c_e}{q_m}$			D–R model $\ln q_e = \ln q_m - \frac{1}{2E^2}[RT\ln(1+\frac{1}{c_e})]^2$		
	K_F	n	R^2	q_m (mg/g)	b (L/mg)	R^2	q_m (mg/g)	E (kJ/mol)	R^2
Single Ni(II)	17.74	0.11	0.985	28.90	0.397	0.998	40.18	14.12	0.974
Ni(II)–Ca(II)	5.72	0.22	0.991	23.49	0.156	0.998	25.48	11.01	0.991
Ni(II)–Fe(III)	3.68	0.33	0.976	17.47	0.0725	0.999	23.79	11.81	0.973
Ni(II)–Cd(II)	1.86	0.36	0.979	11.52	0.0483	0.999	15.77	11.08	0.986
Ni(II)–Pb(II)	0.43	0.53	0.983	7.34	0.0204	0.992	13.83	9.03	0.988
Ni(II)–citrate	10.40	0.15	0.989	20.82	0.209	0.999	27.47	12.68	0.993
Ni(II)–NTA	2.21	0.42	0.990	17.44	0.0516	0.996	21.42	10.48	0.994
Ni(II)–EDTA	1.06	0.45	0.993	11.25	0.0266	0.999	14.95	9.89	0.994

four cations coexisting systems follows the trend of Ni(II)–Ca(II) > Ni(II)–Fe(III) > Ni(II)–Cd(II) > Ni(II)–Pb(II), indicating that the highest interference of Pb(II), followed by Cd(II), Fe(III) and Ca(II) in turn. Similarly, the parameter b for the above three complexing reagents coexistent systems is in order of Ni(II)–citrate > Ni(II)–NTA > Ni(II)–EDTA, suggesting that EDTA shows a more significant influence on Ni(II) adsorption than citrate and NTA. The value of $1/n$ derived from the Freundlich model is smaller than 1, which indicates that Ni(II) is easily adsorbed by the chelating membrane. It should be noted that the value of E for all adsorption systems analyzed by the D–R isotherm model varies in the range of 8–16 kJ/mol, indicating the chemisorption characteristic of Ni(II) adsorption by the chelating membrane [5,56].

In addition, the thermodynamic parameters including standard free energy change ($\Delta G°$), standard enthalpy change ($\Delta H°$) and standard entropy change ($\Delta S°$) were employed to evaluate the adsorption nature of the EDTMPA–TBOT/PVDF membrane toward Ni(II). The calculated values of $\Delta G°$, $\Delta H°$ and $\Delta S°$ were summarized in Table 5. The negative $\Delta H°$ and $\Delta G°$ indicate that Ni(II) adsorption is an exothermic and spontaneous process [38,57]. The positive $\Delta S°$ shows the slight increase in randomness during adsorption process, which may be attributed to the release of water molecules from the hydrated nickel ions.

3.5. Analysis of breakthrough curves

The breakthrough curves were obtained by varying of the thickness of the EDTMPA–TBOT/PVDF membrane stack (0.8, 1.07 and 1.34 mm) for single Ni(II), and four cations and three complexing reagents coexisting systems. During the tests, the concentrations of Ni(II) and all coexisting specimens were kept at 1.0 mmol/L. The flow rate of influent was fixed at 0.128 cm/min, the operating pressure was 20 kPa. The determined TMP values of membrane stacks at Z = 0.8, 1.07 and 1.34 mm were 8, 10 and 15 kPa; thus, TMP rises with the increase in thickness of the membrane stack. Among the eight systems with the same membrane-stacked thickness, the differences in operating pressure and TMP can be ignored. Breakthrough curves of these eight systems are shown in Fig. 10. As evidenced by Fig. 10, all breakthrough curves exhibit an S-shaped character. The values of breakthrough time (t_b, the position at c/c_0 = 0.05) as well as the exhaustion time (t_e, the position at c/c_0 = 0.9) [40,41] can be obtained from these curves (Table 6). The extended trends of t_b and t_e can be observed when the thickness of the membrane stack increases from 0.8 to 1.34 mm. In addition, compared with the single Ni(II) system, the t_b and t_e are shortened at the presence of Ca(II), Fe(III), Cd(II), Pb(II), citrate, NTA and EDTA. Values of t_b and t_e for the membrane stack with the same thickness descend in the order: Ni(II)–citrate > Ni(II)–Ca(II) > Ni(II)–Fe(III) > Ni(II)–NTA > Ni(II)–Cd(II) > Ni(II)–EDTA > Ni(II)–Pb(II), suggesting the remarkable disturbances of EDTA and Pb(II). The plots of breakthrough time against the thickness of membrane stack for the eight systems are all linear ($R^2 > 0.99$), indicating the validity of BDST model for the present eight systems.

Parameters of N_0 and K_a can be calculated from the slope and intercept of the BDST plot, the values of them are also shown in Table 6. With the presence of Ca(II), Fe(III), Cd(II) and Pb(II), the decrease in N_0 value validates the negative effects of these cations on the Ni(II) uptake. The order of N_0 is Ni(II) > Ni(II)–Ca(II) > Ni(II)–Fe(III) > Ni(II)–Cd(II) > Ni(II)–Pb(II), indicating that Pb(II) shows a higher interference than other three cations. The decrease in N_0 with the presence of citrate, NTA and EDTA is manifested, also showing the interferences of these three complexing reagents on the capture of Ni(II), and the detrimental effect of EDTA is most remarkable. In addition, at the presence of cations and complexing reagents, the decrease in K_a value (Table 6) elucidates the requirement of high membrane stack thickness for avoiding breakthrough in the capture of Ni(II). Based on the above analyses, we can confirm the negative effects of coexisting cations and complexing reagents on the Ni(II) adsorption by the EDTMPA–TBOT/PVDF membrane.

3.6. Reuse of the chelating membrane

In this research, 0.5 mol/L of H_2SO_4 solution was adopted to regenerate the chelating membrane. The adsorption/desorption processes were performed 10 times (Fig. 11). After 10 cycles of adsorption/desorption processes, the adsorption capacity of the EDTMPA–TBOT/PVDF membrane is well maintained, the Ni(II) uptake still exceeds 21 mg/g, and the loss of the adsorption capacity is smaller than 10%. Besides, the DE value of the membrane is higher than 93%. Thus,

Table 5
Adsorption thermodynamic parameters of the membrane toward Ni(II) at 298 K

System	$\Delta H°$ (kJ/mol)	$\Delta S°$ (kJ/(mol K))	$\Delta G°$ (kJ/mol)			R^2
			288 K	298 K	308 K	
Single Ni(II)	–14.87	0.0411	–26.71	–27.12	–27.53	0.993
Ni(II)–Ca(II)	–12.52	0.0283	–20.67	–20.95	–21.24	0.994
Ni(II)–Fe(III)	–10.79	0.0249	–17.96	–18.21	–18.46	0.998
Ni(II)–Cd(II)	–8.14	0.0263	–15.71	–15.98	–16.24	0.990
Ni(II)–Pb(II)	–7.31	0.0186	–12.67	–12.85	–13.04	0.998
Ni(II)–citrate	–13.26	0.0342	–23.11	–23.45	–23.79	0.992
Ni(II)–NTA	–8.77	0.0238	–15.62	–15.86	–16.10	0.993
Ni(II)–EDTA	–7.56	0.0216	–13.78	–14.00	–14.21	0.998

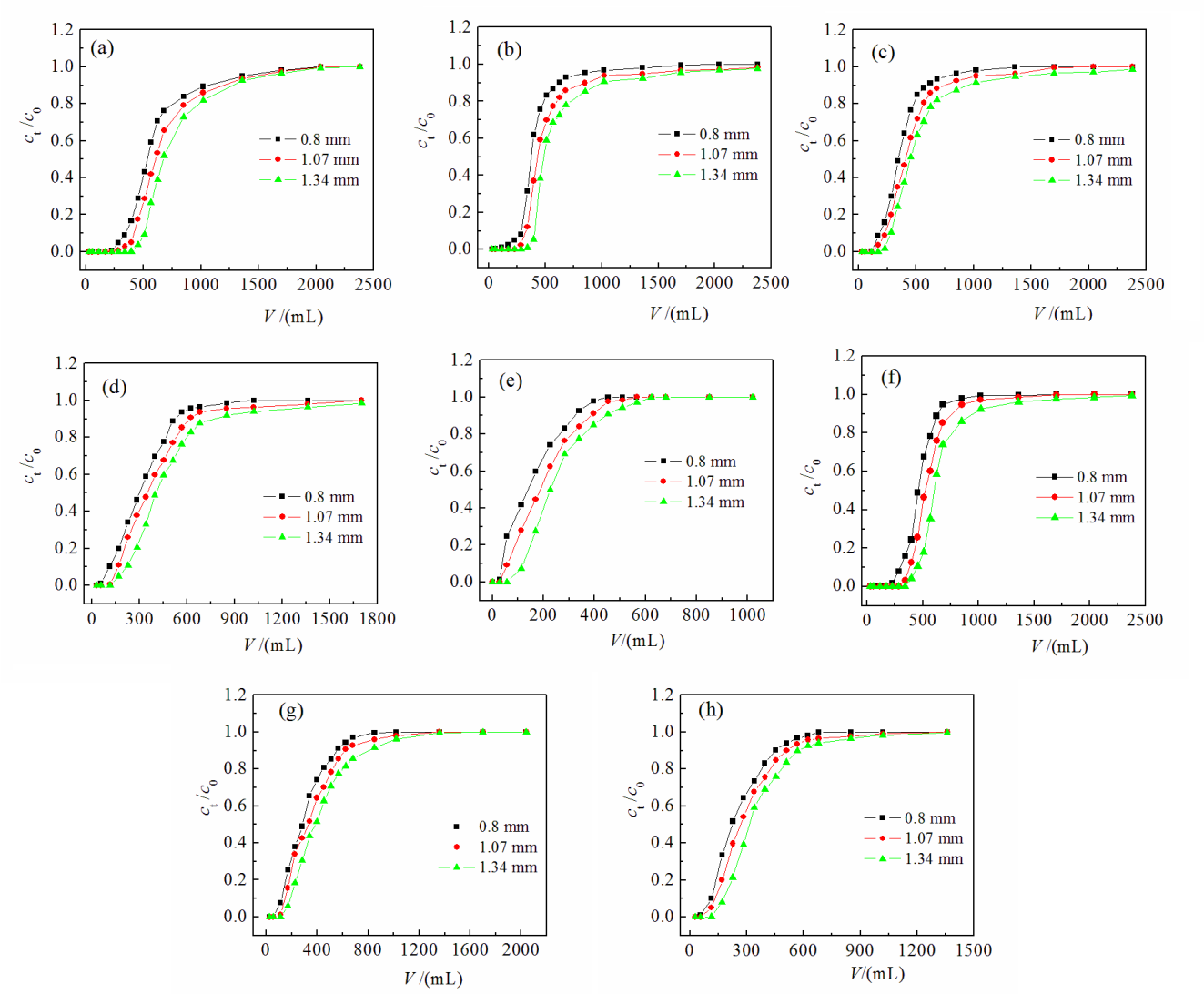

Fig. 10. The breakthrough curves of chelating membrane toward Ni(II): (a) single Ni(II) system; (b) Ni(II)–Ca(II) system; (c) Ni(II)–Fe(III) system; (d) Ni(II)–Cd(II) system; (e) Ni(II)–Pb(II) system; (f) Ni(II)–citrate system; (g) Ni(II)–NTA system and (h) Ni(II)–EDTA system. c_0(Ni(II)) = c_0(Ca(II)) = c_0(Fe(III)) = c_0(Cd(II)) = c_0(Pb(II)) = c_0(citrate) = c_0(NTA) = c_0(EDTA) = 1.0 mmol/L; T: 298 K; flow rate: 0.128 cm/min; pH: 5.4.

the chelating membrane can be repeatedly used for the removal of Ni(II) from aqueous solutions on account of the insignificant loss of Ni(II) uptake.

4. Conclusions

The fabricated EDTMPA–TBOT/PVDF chelating membrane was employed to remove Ni(II) from the aqueous solution. The behavior of this chelating membrane toward Ni(II) was investigated at the presence of Ca(II), Fe(III), Cd(II), Pb(II), citrate, NTA and EDTA. The conclusions are shown as follows:

- The interferential influence of Pb(II) on the Ni(II) adsorption is higher than those of Ca(II), Fe(III) and Cd(II); EDTA shows a more detrimental effect on the Ni(II) uptake than citrate and NTA.
- The presence of coexisting cations and complexing reagents does not alter the adsorption nature of the chelating membrane toward Ni(II). The Lagergren second-order equation and the Langmuir model are suitable for the descriptions in the adsorption kinetics, and the adsorption isotherms. The adsorption of Ni(II) by the chelating membrane is a spontaneous and exothermic process.
- The chelating membrane shows an excellent reuse property, thereby exhibiting a potential application for the recovery of Ni(II) from the aqueous solution.

Acknowledgments

This work was supported by the Scientific Research Foundation of the Hebei Higher Education Institutions of

Table 6
Analyzed parameters of breakthrough curves for the chelating membrane toward Ni(II) at 298 K

System	Z (mm)	t_b (min)	t_e (min)	BDST model		
				N_0 (mmol/L)	K_a (L/min mmol)	R^2
Single Ni(II)	0.8	50.4	188.1	86.5	0.87	0.999
	1.07	69.3	212.5			
	1.34	86.9	225.4			
Ni(II)–Ca(II)	0.8	40.5	108.7	70.6	0.77	0.997
	1.07	54.9	142.8			
	1.34	70.3	176.6			
Ni(II)–Fe(III)	0.8	24.7	105.9	46.7	0.70	0.998
	1.07	35.4	132.9			
	1.34	44.4	168.8			
Ni(II)–Cd(II)	0.8	15.6	92.4	33.2	0.60	0.998
	1.07	23.3	108.6			
	1.34	29.6	136.1			
Ni(II)–Pb(II)	0.8	7.6	57.3	20.9	0.51	0.999
	1.07	10.9	68.2			
	1.34	16.4	78.5			
Ni(II)–citrate	0.8	45.1	115.9	78.7	0.78	0.998
	1.07	62.7	147.8			
	1.34	78.3	183.7			
Ni(II)–NTA	0.8	17.5	98.2	35.8	0.62	0.998
	1.07	25.4	109.0			
	1.34	32.6	142.3			
Ni(II)–EDTA	0.8	13.2	79.8	30.1	0.56	0.997
	1.07	20.7	90.2			
	1.34	25.9	101.9			

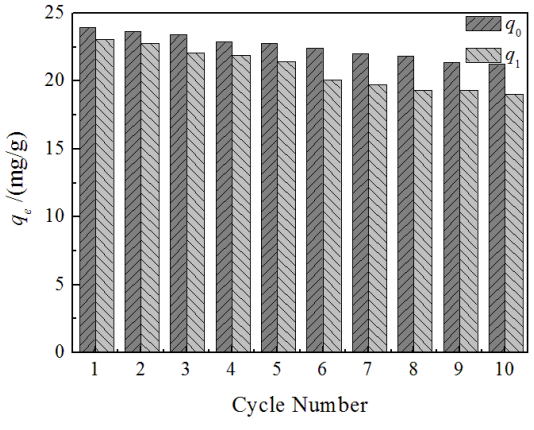

Fig. 11. Adsorption/desorption behavior of the EDTMPA–TBOT/PVDF membrane.

China (Grant No. ZD2015120) and the Hebei Provincial Natural Science Foundation of China (Grant No. B2016203012). Herein, we are also very grateful to the editors and the reviewers for giving the valuable and instructive comments.

References

[1] M. Cempel, G. Nikel, Nickel: a review of its sources and environmental toxicology, Pol. J. Environ. Stud., 15 (2006) 375–382.
[2] K.E. Giller, E. Witter, S.P. Mcgrath, Toxicity of heavy metals to microorganisms and microbial processes in agricultural soils: a review, Soil Biol. Biochem., 30 (1998) 1389–1414.
[3] L. Wang, R.T. Liu, Y. Teng, Study on the toxic interactions of Ni^{2+} with DNA using neutral red dye as a fluorescence probe, J. Lumin., 131 (2011) 705–709.
[4] L. Shi, J.S. Shi, Y. Shi, Discussion on the emission standard of pollutants for electroplating, Electroplat. Finish., 60 (2009) 590–594.
[5] L.Z. Song, M. Yang, J. Fu, P.P. Lu, X.L. Wang, J. He, Adsorption performance of APTMS-DTPA/PVDF chelating membrane toward Ni(II) with the presence of Ca(II), NH_4^+, lactic acid, and citric acid, Desal. Wat. Treat., 53 (2015) 158–170.
[6] A.H. Elshazly, A.H. Konsowa, Removal of nickel ions from wastewater using a cation-exchange resin in a batch-stirred tank reactor, Desalination, 158 (2003) 189–193.
[7] W.C. Ying, R.R. Bonk, M.E. Tucker, Precipitation treatment of spent electroless nickel plating baths, J. Hazard. Mater., 18 (1988) 69–89.
[8] M.A. Hanif, R. Nadeem, H.N. Bhatti, N.R. Ahmad, T.M. Ansari, Ni(II) biosorption by *Cassia fistula* (Golden Shower) biomass, J. Hazard. Mater., 139 (2007) 345–355.
[9] P. Sanciolo, I.H. Harding, D.E. Mainwaring, The removal of chromium, nickel, and zinc from electroplating wastewater

by adsorbing colloid flotation with a sodium dodecylsulfate/dodecanoic acid mixture, Sep. Sci. Technol., 27 (1992) 375–388.
[10] K. Dermentzis, A. Christoforidis, E. Valsamidou, Removal of nickel, copper, zinc and chromium from synthetic and industrial wastewater by electrocoagulation, Int. J. Environ. Sci., 1 (2011) 697–710.
[11] J.E. Silva, A.P. Paiva, D. Soares, A. Labrincha, F. Castro, Solvent extraction applied to the recovery of heavy metals from galvanic sludge, J. Hazard. Mater., 120 (2005) 113–118.
[12] B.S. Gupta, M. Curran, S. Hasan, T.K. Ghosh, Adsorption characteristics of Cu and Ni on Irish peat moss, J. Environ. Manage., 90 (2009) 954–960.
[13] Q. Li, H.J. Su, J. Li, T.W. Tan, Application of surface molecular imprinting adsorbent in expanded bed for the adsorption of Ni^{2+} and adsorption model, J. Environ. Manage., 85 (2007) 900–907.
[14] D. Nabarlatz, J.D. Celis, P. Bonelli, A.L. Cukierman, Batch and dynamic sorption of Ni(II) ions by activated carbon based on a native lignocellulosic precursor, J. Environ. Manage., 97 (2012) 109–115.
[15] A. Ewecharoen, P. Thiravetyan, E. Wendel, H. Bertagnolli, Nickel adsorption by sodium polyacrylate-grafted activated carbon, J. Hazard. Mater., 171 (2009) 335–339.
[16] E. Pehlivan, G. Arslan, Removal of metal ions using lignite in aqueous solution—low cost biosorbents, Fuel Process. Technol., 88 (2007) 99–106.
[17] M. Saleem, N. Wongsrisujarit, S. Boonyarattanakalin, Removal of nickel (II) ion by adsorption on coconut copra meal biosorbent, Desal. Wat. Treat., 57 (2016) 5623–5635.
[18] P.P. Vishvakarma, K.P. Yavada, V. Singh, Nickel (II) removal from aqueous solutions by adsorption on fly-ash, Pertanika, 12 (1989) 357–366.
[19] A.I. Zouboulis, K.A. Kydros, Use of red mud for toxic metals removal: the case of nickel, J. Chem. Technol. Biotechnol., 58 (1993) 95–101.
[20] S.S. Gupta, K.G. Bhattacharyya, Immobilization of Pb(II), Cd(II) and Ni(II) ions on kaolinite and montmorillonite surfaces from aqueous medium, J. Environ. Manage., 87 (2008) 46–58.
[21] S. Çoruh, O.N. Ergun, Ni^{2+} removal from aqueous solutions using conditioned clinoptilolites: kinetic and isotherm studies, Environ. Prog. Sustainable Energy, 28 (2009) 162–172.
[22] T. Becker, M. Schlaak, H. Strasdeit, Adsorption of nickel(II), zinc(II) and cadmium(II) by new chitosan derivatives, React. Funct. Polym., 44 (2000) 289–298.
[23] Y. Vijaya, S.R. Popuri, V.M. Boddu, A. Krishnaiah, Modified chitosan and calcium alginate biopolymer sorbents for removal of nickel (II) through adsorption, Carbohydr. Polym., 72 (2008) 261–271.
[24] G. Arthanareeswaran, P. Thanikaivelan, J.A. Raguime, M. Raajenthiren, D. Mohan, Metal ion separation and protein removal from aqueous solutions using modified cellulose acetate membranes: role of polymeric additives, Sep. Purif. Technol., 55 (2007) 8–15.
[25] B. Kalbfuss, M. Wolff, L. Geisler, A. Tappe, R. Wickramasinghe, V. Thom, U. Reichl, Direct capture of influenza A virus from cell culture supernatant with Sartobind anion-exchange membrane adsorbers, J. Membr. Sci., 299 (2007) 251–260.
[26] K. Dermentzis, Removal of nickel from electroplating rinse waters using electrostatic shielding electrodialysis/electrodeionization, J. Hazard. Mater., 173 (2010) 647–652.
[27] R.A. Kumbasar, S. Kasap, Selective separation of nickel from cobalt in ammoniacal solutions by emulsion type liquid membranes using 8-hydroxyquinoline (8-HQ) as mobile carrier, Hydrometallurgy, 95 (2009) 121–126.
[28] M.A. Barakat, E. Schmidt, Polymer-enhanced ultrafiltration process for heavy metals removal from industrial wastewater, Desalination, 256 (2010) 90–93.
[29] A.W. Mohammad, R. Othaman, N. Hilal, Potential use of nanofiltration membranes in treatment of industrial wastewater from Ni–P electroless plating, Desalination, 168 (2004) 241–252.
[30] L.A. Richards, B.S. Richards, A.I. Schäfer, Renewable energy powered membrane technology: salt and inorganic contaminant removal by nanofiltration/reverse osmosis, J. Membr. Sci., 369 (2011) 188–195.
[31] S.B. Deng, Y.P. Ting, Characterization of PEI-modified biomass and biosorption of Cu(II), Pb(II) and Ni(II), Water Res., 39 (2005) 2167–2177.
[32] A. Baraka, P.J. Hall, M.J. Heslop, Preparation and characterization of melamine–formaldehyde–DTPA chelating resin and its use as an adsorbent for heavy metals removal from wastewater, React. Funct. Polym., 67 (2007) 585–600.
[33] H. Yoo, S.Y. Kwak, Surface functionalization of PTFE membranes with hyperbranched poly(amidoamine) for the removal of Cu^{2+} ions from aqueous solution, J. Membr. Sci., 448 (2013) 125–134.
[34] C.S. Zhao, X.S. Zhou, Y.L. Yue, Determination of pore size and pore size distribution on the surface of hollow-fiber filtration membranes: a review of methods, Desalination, 129 (2000) 107–123.
[35] Lj.S. Čerović, S.K. Milonjić, M.B. Todorović, M.I. Trtanj, Y.S. Pogozhev, Y. Blagoveschenskii, E.A. Levashov, Point of zero charge of different carbides, Colloids Surf., A, 297 (2007) 1–6.
[36] X.L. Wang, L.Z. Song, F.F. Yang, J. He, Investigation of phosphate adsorption by a polyethersulfone-type affinity membrane using experimental and DFT methods, Desal. Wat. Treat., 57 (2016) 25036–25056.
[37] X.D. Zhao, L.Z. Song, J. Fu, P. Tang, F. Liu, Adsorption characteristics of Ni(II) onto MA–DTPA/PVDF chelating membrane, J. Hazard. Mater., 189 (2011) 732–740.
[38] L.Z. Song, R.F. Zhao, D.D. Yun, P.P. Lu, J. He, X.L. Wang, Influence of Co(II), Ni(II), tartrate, and ethylenediaminetetraacetic acid on Cu(II) adsorption onto a polyvinylidene fluoride-based chelating membrane, Toxicol. Environ. Chem., 96 (2014) 362–378.
[39] G.S. Bohart, E.Q. Adams, Some aspects of the behavior of charcoal with respect to chlorine, J. Am. Chem. Soc., 42 (1920) 523–544.
[40] M. Ghasemi, A.R. Keshtkar, R. Dabbagh, S.J. Safdari, Biosorption of uranium(VI) from aqueous solutions by Ca-pretreated *Cystoseira indica* alga: breakthrough curves studies and modeling, J. Hazard. Mater., 189 (2011) 141–149.
[41] X. Zhang, H.J. Su, T.W. Tan, G. Xiao, Study of thermodynamics and dynamics of removing Cu(II) by biosorption membrane of penicillium biomass, J. Hazard. Mater., 193 (2011) 1–9.
[42] C. Chen, C.H. Shen, G.J. Kong, S.J. Gao, High temperature proton exchange membranes prepared from epoxycyclohexylethyltrimethoxysilane and amino trimethylene phosphonic acid as anhydrous proton conductors, Mater. Chem. Phys., 140 (2013) 24–30.
[43] J.F. Xu, X.Y. Wu, G.T. Fu, X.Y. Liu, Y. Chen, Y.M. Zhou, Y.W. Tang, T.H. Lu, Fabrication of phosphonate functionalized platinum nanoclusters and their application in hydrogen peroxide sensing in the presence of oxygen, Electrochim. Acta, 80 (2012) 233–239.
[44] T.Y. Ma, H. Li, A.N. Tang, Z.Y. Yuan, Ordered, mesoporous metal phosphonate materials with microporous crystalline walls for selective separation techniques, Small, 13 (2011) 1827–1837.
[45] T.Y. Ma, X.J. Zhang, Z.Y. Yuan, Hierarchically meso-/macroporous titanium tetraphosphonate materials: synthesis, photocatalytic activity and heavy metal ion adsorption, Microporous Mesoporous Mater., 123 (2009) 234–242.
[46] N. Ferrah, O. Abderrahim, M.A. Didi, D. Villemin, Removal of copper ions from aqueous solutions by a new sorbent: polyethyleneiminemethylene phosphonic acid, Desalination, 269 (2011) 17–24.
[47] X.S. Luo, Z. Zhang, P.X. Zhou, Y.N. Liu, G.F. Ma, Z.Q. Lei, Synergic adsorption of acid blue 80 and heavy metal ions (Cu^{2+}/Ni^{2+}) onto activated carbon and its mechanisms, J. Ind. Eng. Chem., 27 (2015) 164–174.
[48] G.M. Qiu, L.P. Zhu, B.K. Zhu, Y.Y. Xu, G.L. Qiu, Grafting of styrene/maleic anhydride copolymer onto PVDF membrane by supercritical carbon dioxide: preparation, characterization and biocompatibility, J. Supercrit. Fluids, 45 (2008) 374–383.
[49] V.L. Silva, R. Carvalho, M.P. Freitas, C.F. Tormena, W.C. Melo, Structural determination of Zn and Cd–DTPA complexes: MS, infrared, ^{13}C NMR and theoretical investigation, Spectrochim. Acta, Part A, 68 (2007) 1197–1200.

[50] H.M. Kao, C.H. Liao, A. Palani, Y.C. Liao, One-pot synthesis of ordered and stable cubic mesoporous silica SBA-1 functionalized with amino functional groups, Microporous Mesoporous Mater., 113 (2008) 212–223.
[51] M.W. McKittrick, C.W. Jones, Toward single-site functional materials preparation of amine-functionalized surfaces exhibiting site-isolated behavior, Chem. Mater. 15 (2003) 1132–1139.
[52] D.D. Zheng, J.F. Zhou, L. Zhong, F.X. Zhang, G.X. Zhang, A novel durable and high-phosphorous-containing flame retardant for cotton fabrics, Cellulose, 23 (2016) 2211–2220.
[53] H. Lata, V.K. Garg, R.K. Gupta, Sequestration of nickel from aqueous solution onto activated carbon prepared from *Parthenium hysterophorus* L., J. Hazard. Mater., 157 (2008) 503–509.
[54] Y. Hannachi, N.A. Shapovalov, A. Hannachi, Adsorption of nickel from aqueous solution by the use of low-cost adsorbents, Korean J. Chem. Eng., 27 (2010) 152–158.
[55] B.P. Bering, M.M. Dubinin, V.V. Serpinsky, On thermodynamics of adsorption in micropores, J. Colloid Interface Sci., 38 (1972) 185–194.
[56] M.V. Dinu, E.S. Dragan, Heavy metals adsorption on some iminodiacetate chelating resins as a function of the adsorption parameters, React. Funct. Polym., 68 (2008) 1346–1354.
[57] A. Ramesh, D.J. Lee, J.W.C. Wong, Thermodynamic parameters for adsorption equilibrium of heavy metals and dyes from wastewater with low-cost adsorbents, J. Colloid Interface Sci., 291 (2005) 588–592.